Electronic Supplementary Material (ESI) for Nanoscale.

Supplementary Information

Vertically Integrated Visible and Near-Infrared Metasurfaces Enabling an Ultra-Broadband and Highly Angle-Resolved Anomalous Reflection

Song Gao,[a] Sang-Shin Lee,*[a] Eun-Soo Kim,[a] and Duk-Yong Choi[b]

[a]Department of Electronic Engineering, Kwangwoon University, 20 Kwangwoon-ro, Nowon-gu, Seoul 01897, South Korea

[b]Laser Physics Centre, Research School of Physics and Engineering, Australian National University, Canberra ACT 2601, Australia

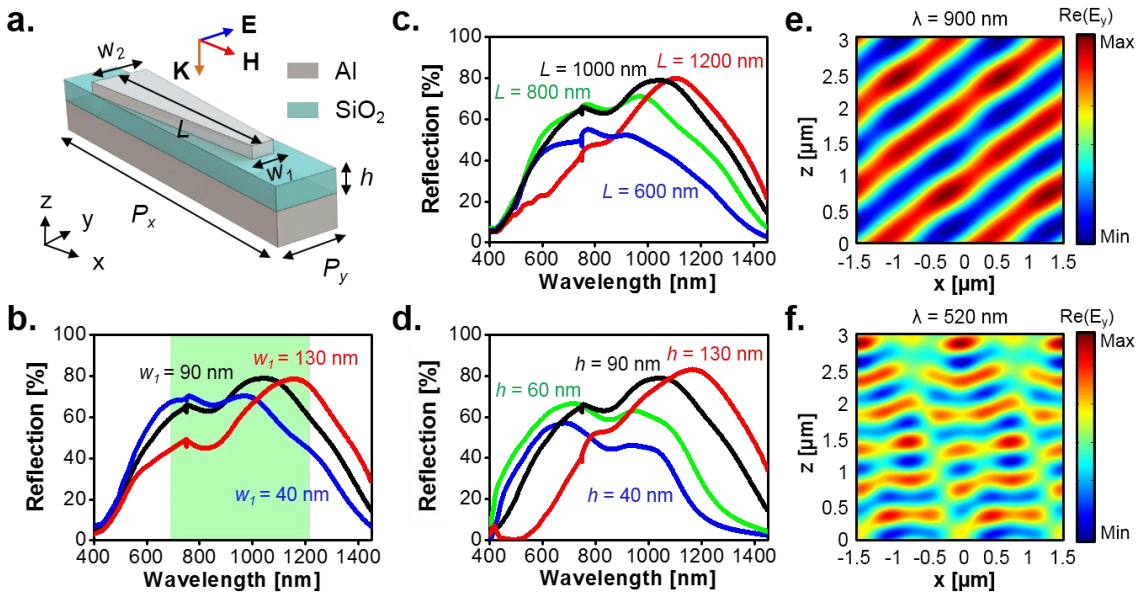

Figure S1. (a) Metasurface with the supercell consisting of a single trapezoidal Al antenna. Dependence of the -1st order diffraction spectral response on (b) the antenna width w_1, (c) the antenna length L, and (d) the dielectric thickness h. Calculated y-component of the reflected electric field (real part) at the wavelengths of (e) 900 nm and (f) 520 nm for normal incidence.

Figure S1(a) shows that for the conventional metasurface tapping into a single Al antenna, the basic structural parameters are P_x = 1500 nm, P_y = 250 nm, L = 1000 nm, h = 90 nm, w_1 = 90 nm, and w_2 = 250 nm. Figures S1(b) through S1(d) plot the calculated anomalous reflection spectra corresponding to the -1st order diffraction as shown in black line, for normally incident light with the electric field aligned parallel to the y-axis. The efficiency, which reaches a maximum of 80% at λ = 1040 nm, is observed to exceed 60% across a spectral bandwidth of Δλ = 500 nm from λ = 700 to around 1200 nm, which translate into moderate reflection angles ranging from -27.8 ° to -53.1 °. The diffraction spectral responses in terms of the width (w_1) and length (L) of the trapezoidal Al and the dielectric thickness (h) have been examined, as included in Figures S1(b), S1(c), and S1(d), respectively. For each case, only the structural parameter of concern is altered with the remainder of the parameters kept constant. As shown in Figure S1(b), with increasing antenna width (w_1), the efficiency gradually decreases from λ = 550 nm to 900 nm but increases after λ = 1100 nm. It seems that the peak position for the efficiency slightly shifts towards the long wavelength region, which is presumed to originate from the red-shift of the gap-plasmon resonance with increasing width of the antenna.[1] No noticeable improvement in the efficiency is monitored in the short VIS band running from λ = 400 nm to 550 nm.

The diffraction characteristic is also relevant to the antenna length and the dielectric thickness, as shown in Figures S1(c) and S1(d). A thicker (thinner) dielectric layer results in a higher efficiency at long (short) wavelength region, as in the case of the previous work.[2] Simply optimizing the parameters of the antenna and the dielectric layer is not expected to drastically expand the spectral bandwidth. The near-field profile at the wavelength 900 nm is depicted in Figure S1(e), assuming a rather planar wavefront propagating at an oblique reflection angle, which is sound evidence of enhanced anomalous reflection. As plotted in Figure S1(f), the wavefront for λ = 520 nm appears to be severely distorted due to the interaction of multiple diffraction orders, which is indicative of a normal reflection.

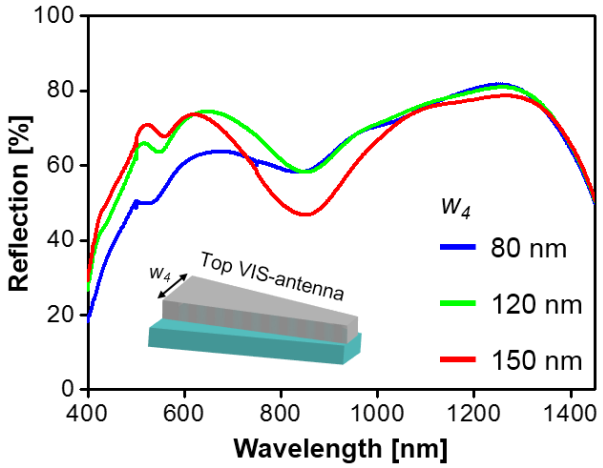

Figure S2. Effect of the width (w_4) of the top VIS-antenna on the anomalous reflection for the case of the proposed metasurface.

In view of the simulation results, a thicker width (w_4) of trapezoid has been recommended to alleviate the efficiency in the visible band, considering that the efficiency however declines in the NIR regime, especially near λ = 880 nm. The width has finally been selected to be 130 nm.

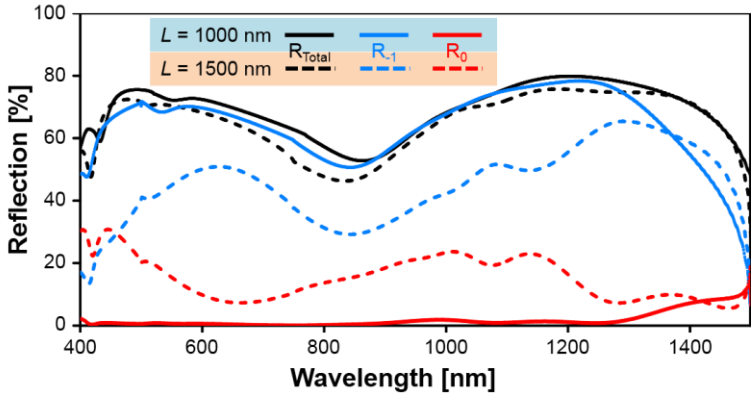

Figure S3. The total reflection (R_{Total}) and diffraction spectra corresponding to the -1st (R_{-1}) and 0th (R_0) orders are calculated for a vertically integrated metasurface with an antenna length of L = 1500 nm. Other structural parameters for the metasurface are kept the same as mentioned in Figure 2a(ii). For comparison, the results from Figure 2a(ii) are also depicted in the figure.

For the vertically integrated metasurface with an antenna length of L = 1500 nm, the total reflection is observed to be similar to that of the case of L = 1000 nm. However, the -1st order diffraction for the former case remarkably decreased compared with the latter one. It is assumed the enhanced 0th order diffraction (R_0) for L = 1500 nm stems from the specular reflection in connection with the embedded NIR-antenna.

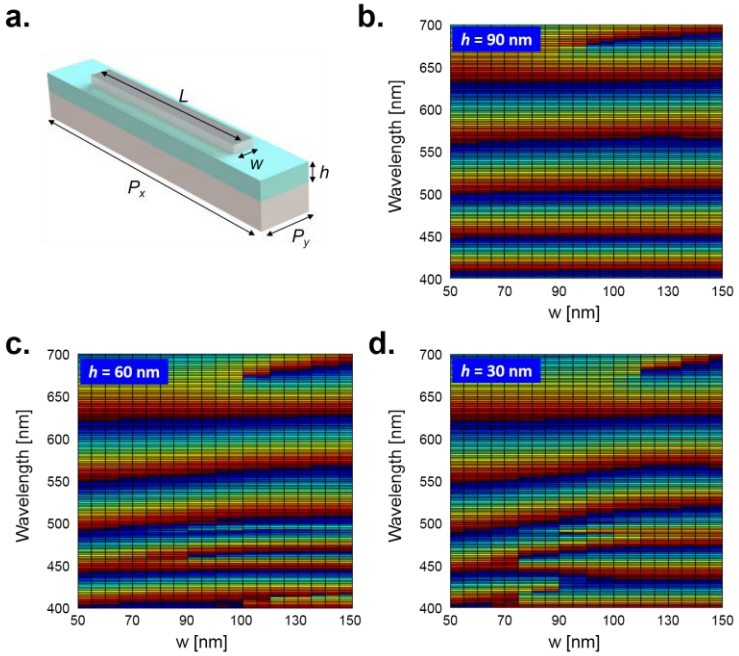

Figure S4. The phase shift in terms of the wavelength and antenna width (w) is theoretically explored for different dielectric thicknesses. (a) Schematic of the conventional metasurface tapping into a single layer of rectangular antenna. The periods are P_x = 1500 nm and P_y = 250 nm; the Al antenna is 40-nm thick, with a length of L = 1000 nm. The phase shift as a function of the antenna width has been calculated for dielectric thicknesses of (b) h = 90 nm, (c) h = 60 nm, and (d) h = 30 nm.

Figure S4(a) sketches the schematic of the conventional gap-plasmonic metasurface involving a single rectangular antenna. The phase shift in the VIS band with respect to the antenna width (w) has been calculated and shown in Figures S4(b), S4(c), and S4(d) for dielectric thicknesses of h = 90 nm, h = 60 nm, and h = 30 nm, respectively. For the antenna width of interest, the phase shift remains relatively stable for the dielectric thickness of h = 90 nm, leading to a low phase gradient. Meanwhile, the phase gradient is observed to increase for thicknesses of h = 60 nm and 30 nm.

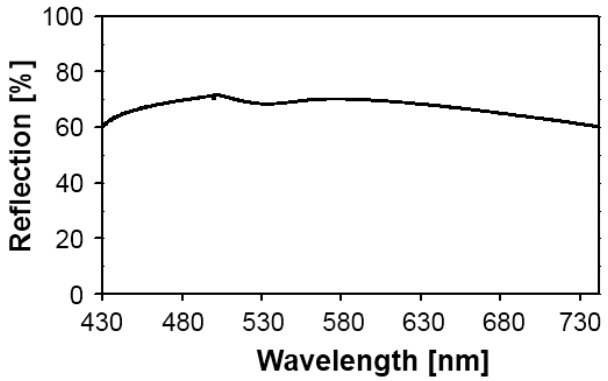

Figure S5. The -1st order diffraction efficiency in the VIS band ranging from λ = 430 nm to 742 nm is extracted from the result given in Figure 2a(ii) of the main text, for the case of the vertically integrated metasurface with the upper SiO_2 thickness of h = 60 nm.

The -1st order diffraction efficiency in the VIS band ranging from λ = 430 nm to 742 nm is particularly depicted in Figure S5. The efficiency corresponding to the abovementioned spectrum stably exceeds 60%.

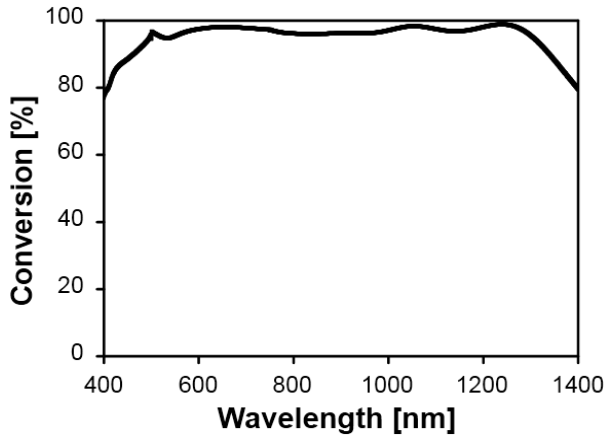

Figure S6. For the proposed metasurface with a 60-nm thick upper SiO_2 layer, the conversion efficiency, defined as the ratio of the anomalous reflection to the total reflection, is calculated, and is found to remain high over an ultra-wide spectral band.

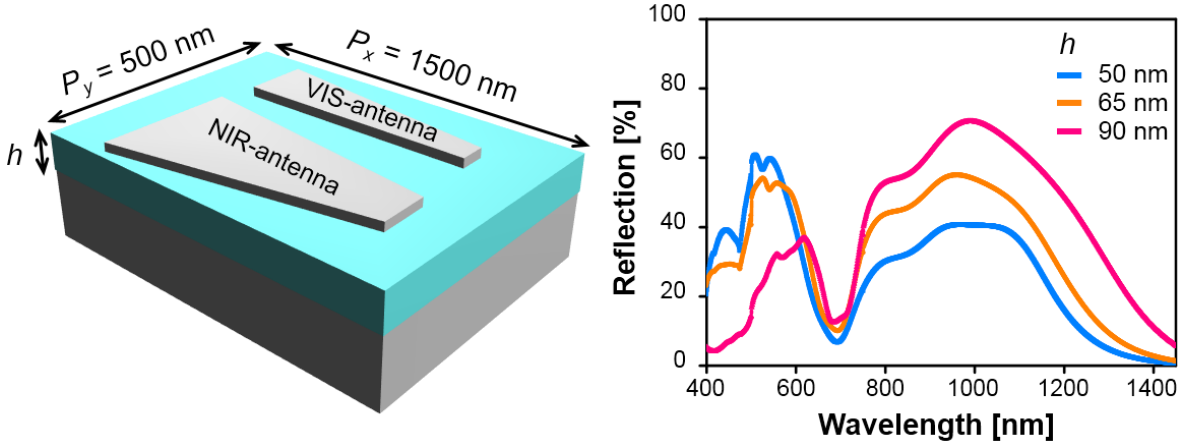

Figure S7. A metasurface design with a co-planar arrangement of the two antennae. One supercell of the metasurface is depicted on the left side. The two antennae are designed with the same parameters as in the main text. The thickness of the SiO_2 dielectric layer affects the anomalous reflection in both the VIS and NIR bands. In this case, an ultra-broadband anomalous reflection obviously cannot be achieved.

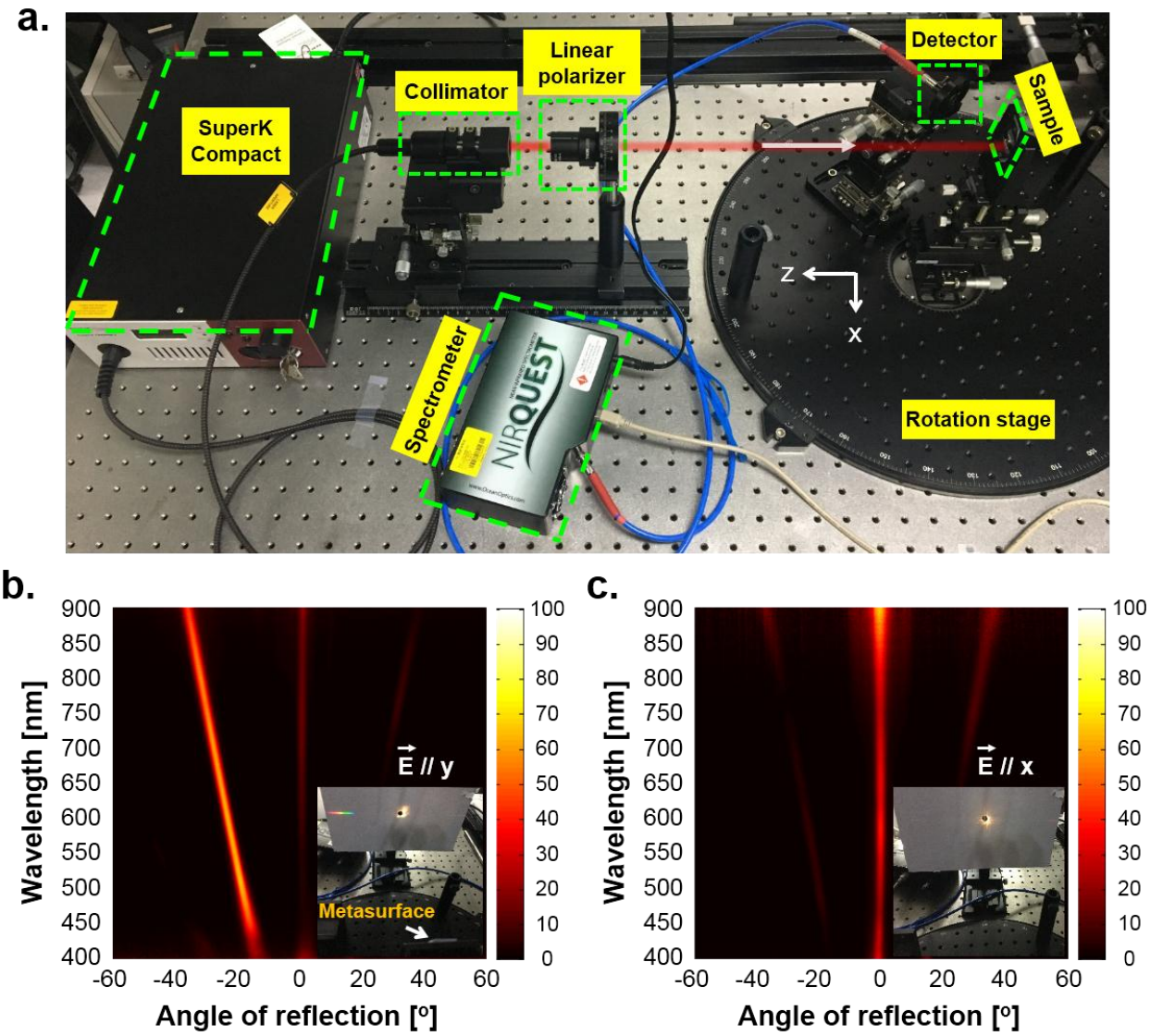

Figure S8. (a) Measurement setup used for capturing the far-field intensity profile in the NIR band. The VIS band far-field intensity distribution for the fabricated sample (80 μm × 80 μm) was recorded by using an FT-ARS system for normally incident light, with the electric field parallel to the (b) y-axis and (c) x-axis. The insets in each figure show the captured reflection images.

The NIR measurement was conducted using a custom-built angle-resolved reflection setup, as shown in Figure S8(a). A supercontinuum laser (NKT SuperK compact) equipped with a collimator is used as the illuminating light source. The emitted light passes through a linear polarizer (GTH10M-A, Thorlabs), and normally impinges on the sample, which is fixed at the center of a rotation stage (RBB450A/M, Thorlabs). Reflected light corresponding to angles ranging both from -90° to -35° and from 35° to 90° is collected by a detector, which is appended to an NIR spectrometer (NIRQuest512-2.5, Ocean Optics) via a fiber. To facilitate the

measurement resorting to the home-built setup, a sample with relatively large dimensions (80 μm × 80 μm) was additionally prepared based on the same design parameters as mentioned in the main text. Prior to commencing the NIR test, the VIS far-field intensity profile for the large sample was first monitored with the FT-ARS system. As shown in Figure S8(b), there is a little deviation compared with the result shown in Figure 5a in the main text, which might be attributed to fabrication errors. It is inferred from the captured reflection image (inset) that the anomalous reflection can be efficiently stimulated for the case of the y-polarization. As displayed in Figure S8(c), no notable anomalous reflection was found under incident light with the polarization parallel to the x-axis, which suggests that the proposed device may work as a polarization beam splitter in the VIS band.

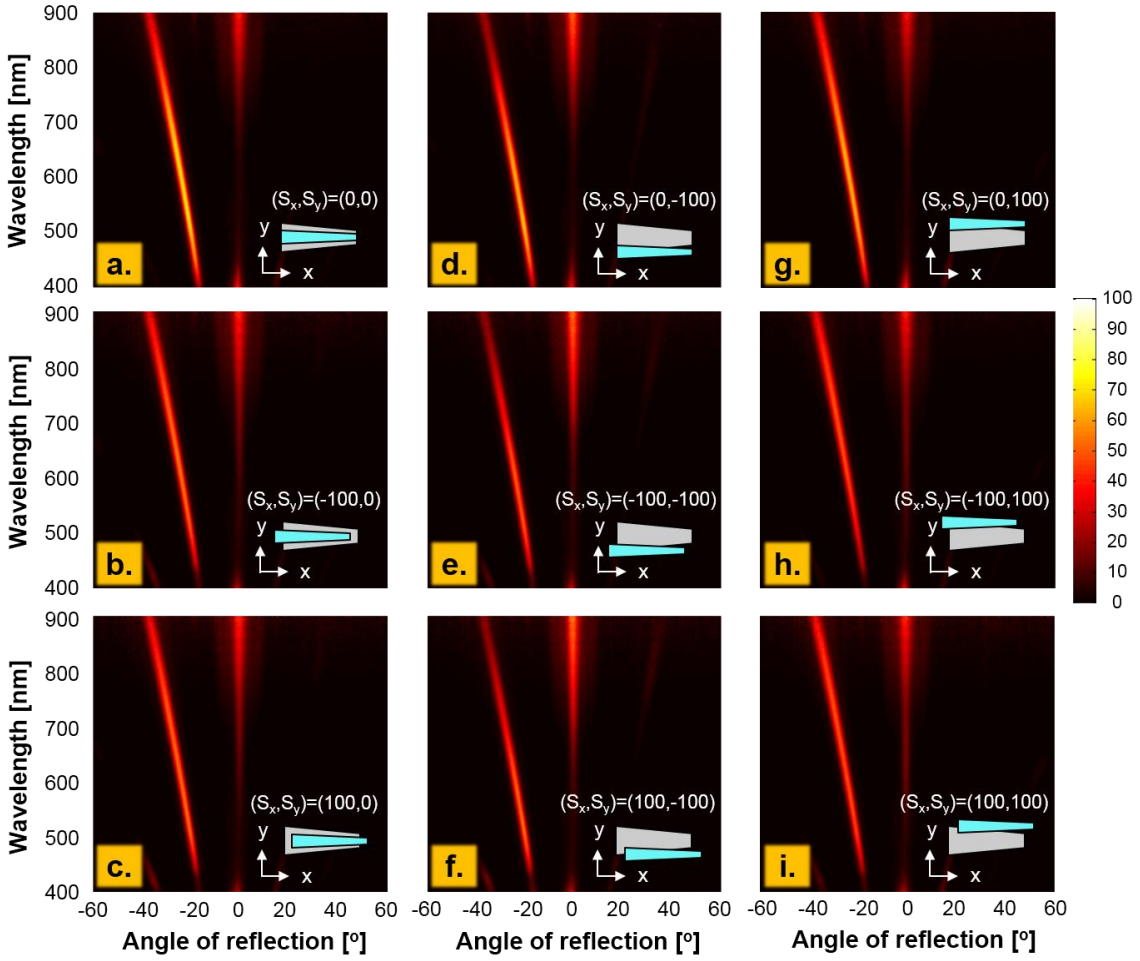

Figure S9. Far-field intensity profiles in the region from λ = 400 nm to 900 nm are obtained from a group of fabricated metasurface devices, when a misalignment of 100 nm is deliberately

introduced, as indicated by the insets. For reference, the measurement result for the proposed metasurface with no misalignment is also plotted in Figure S9(a).

To assess the influence of the misalignment between the top VIS-antenna and the embedded NIR-antenna upon the anomalous reflection, a set of devices with a footprint of 20 μm × 20 μm were prepared, where a 100-nm misalignment is deliberately introduced along the x-direction (S_x) or the y-direction (S_y), as revealed in the Figures S9(a) through S9(i). SEM images for each case are given in Figure S12. The results of the VIS far-field intensity distribution for all the devices revealed that the performance of the designed metasurface is less affected by the y-misalignment, as shown in Figures S9(d) and S9(g). The anomalous reflection is inclined to slightly degrade in the presence of the x-misalignment, as shown in Figures S9(b), S9(c), S9(e), S9(f), S9(h), and S9(i).

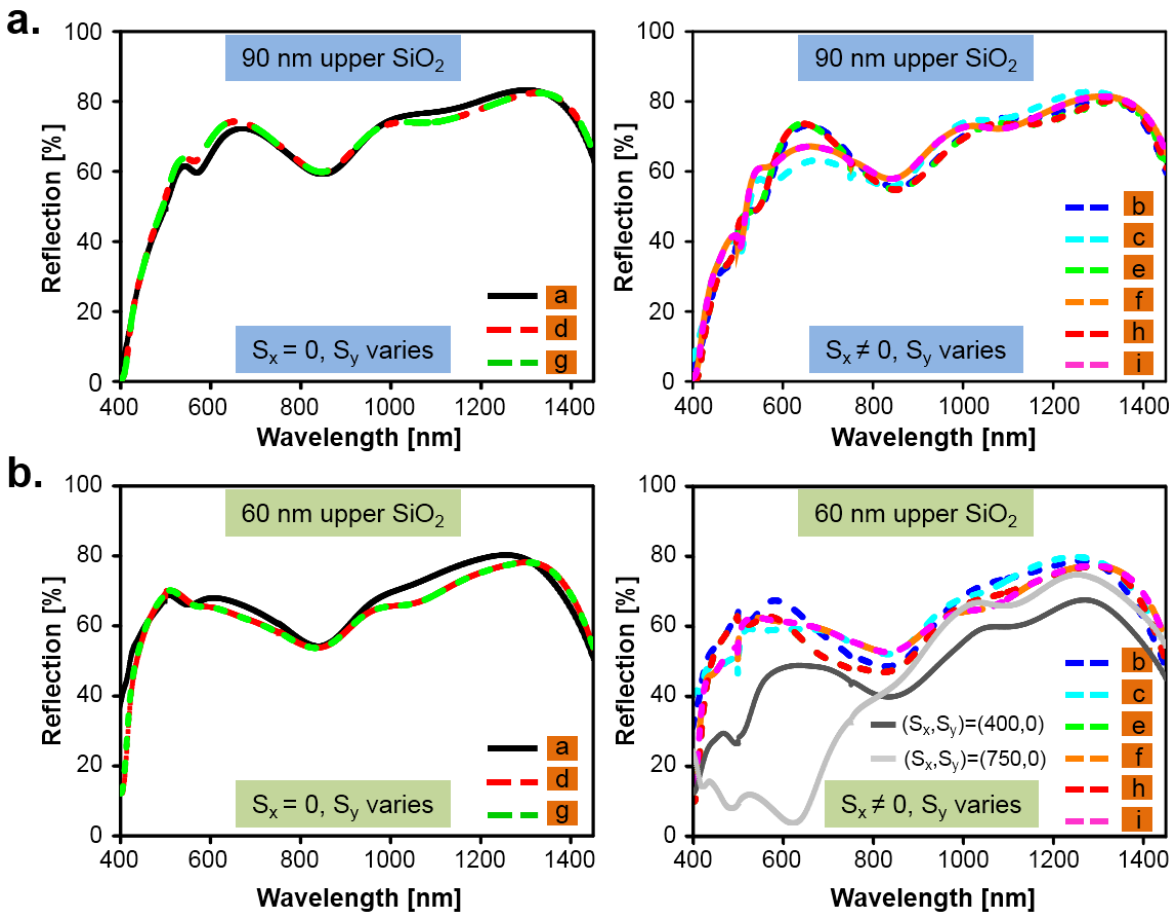

Figure S10. The -1st order diffraction spectra associated with the proposed metasurface are calculated under various misalignment situations. The upper SiO_2 layer belonging to the

metasurface exhibits a flat morphology, while the thickness is determined to be (a) 90 nm and (b) 60 nm.

Simulations are conducted to check the influence of a 100-nm misalignment on the anomalous reflection and relevant results are included in Figure S10. The misalignments for the calculated spectra in solid or dashed lines denoted as "a" through "i" correspond to the misalignments in Figure S9(a) through S9(i), respectively. The metasurface with different thicknesses of upper SiO_2 of (a) h = 90 nm and (b) h = 60 nm has been considered with respect to its -1st order diffraction spectrum. The proposed metasurface gives rise to stable performance as against the induced misalignments, which is in good agreement with the demonstrated results given in Figure S9. The diffraction spectral response appears to remain stable when only the y-misalignment (S_x = 0) is involved, while its efficiency slightly degrades when the x-misalignment is introduced. This trend is invariant to the thickness of the upper SiO_2. The VIS reflection efficiency under large misalignments, (like S_x = 400 nm and 750 nm, as sketched in gray lines in Figure S10(b)), is detrimentally impacted, implying that the progressively varying resonance mode for the top VIS-antenna, which determines the anomalous reflection, has vanished.

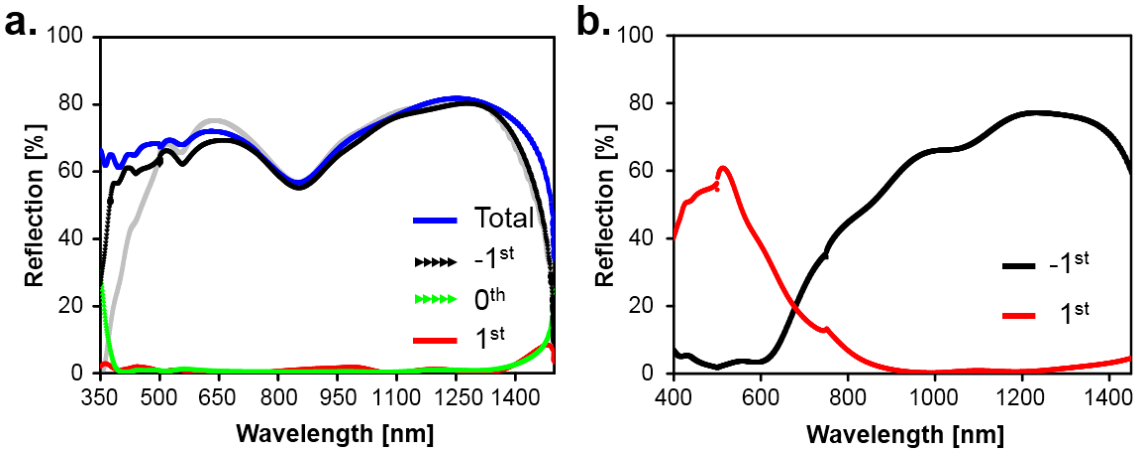

Figure S11. (a) Simulated total reflection and diffraction spectra for different orders, when another metal-dielectric layer is added atop the top VIS-antenna of the proposed metasurface. The gray line represents the -1st order diffraction spectrum for the designed metasurface in the main text. (b) Reflection characteristic for a vertically integrated metasurfaces that is useful for directing the VIS and NIR light into opposite diffraction orders.

When another trapezoidal Al (length of 1000 nm, base widths of 80 nm and 20 nm) in conjunction with a 40-nm thick SiO_2 film of the same shape are added to the VIS-antenna of the proposed metasurface, the -1st order diffraction is further broadened as shown in Figure S11(a). The -1st order diffraction delivers an efficiency exceeding 50% in the spectral range of λ = 374 nm to 1462 nm, closely mimicking the total reflection. Thus, the reflection corresponding to both the 1st and 0th orders are deemed to be negligibly small. The vertically cascaded configuration can also be used to embody a metasurface rendering directional spectrum splitting. When the orientation of the top Al antenna is reversed with reference to that of the embedded Al antenna, the VIS and NIR beams are routed into opposite diffraction orders, as shown in Figure S11(b). This sort of device will be popularly applied to benefit photovoltaic devices.

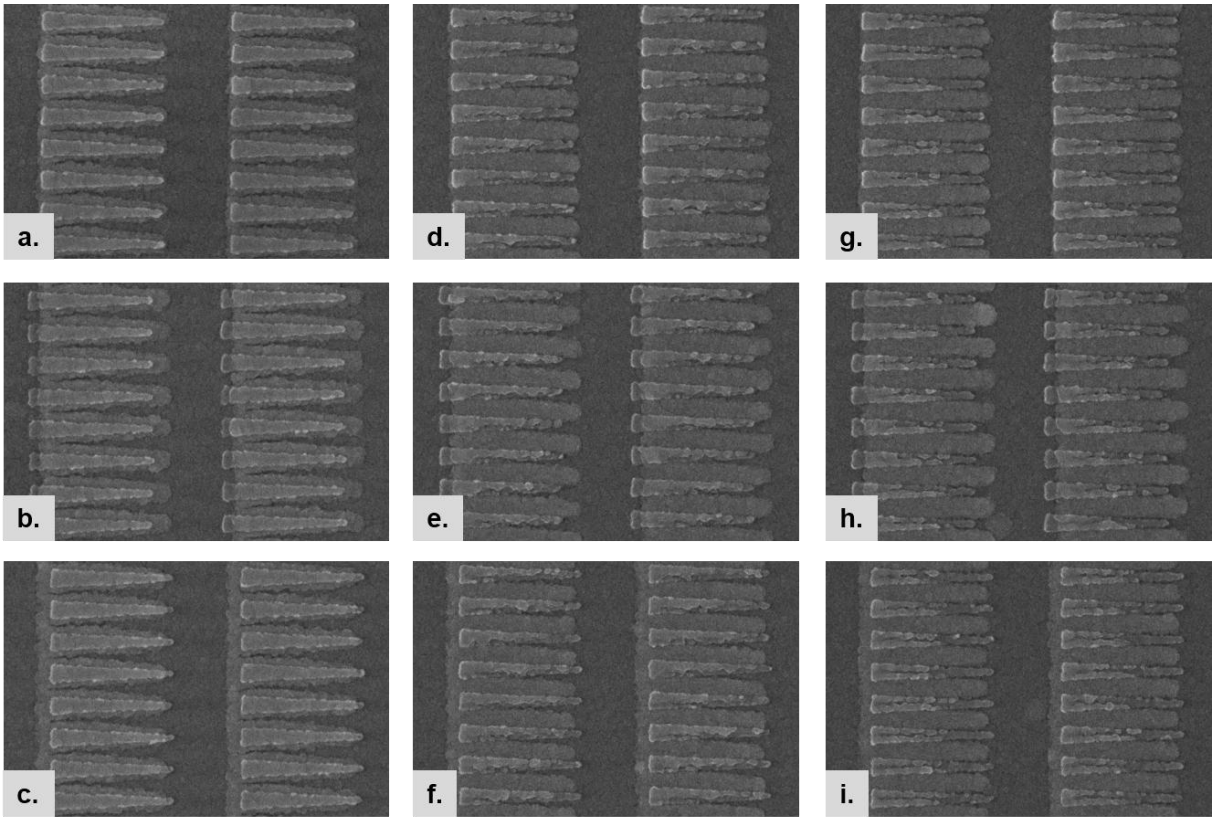

Figure S12. SEM images for the insets of Figure S9.

Reference

[1] Pors, A.; Bozhevolnyi, S. I. *Opt. Express* **2013**, 21, 27438.
[2] Forouzmand, A.; Mosallaei, H. *J. Nanophoton.* **2017**, 11, 010501.